RSC Advances




ROYAL SOCIETY OF CHEMISTRY

www.rsc.org/advances

# Effect of co-crystallization of ethanol, pyridine and 2,2'-bipyridine on molecular aggregation in bis(1,2,3,4-tetrahydroquinolinedithiocarbamato-S,S')mercury(II) and synthesis of HgS nanoparticles

**Narayanaswamy Srinivasan[a], Subbiah Thirumaran*[a] and Samuele Ciattini[b]**
[a] *Department of Chemistry, Annamalai University, Annamalinagar 608 002, Tamilnadu, India*
[b] *Centro di Cristallografia Strutturale, Polo Scientifio di Sesto Fiorentino, Via della Lastruccia N°3, 50019 Sesto Fiorentino, Firenze, Italy*



* Corresponding author. Tel.: +91 9842897597.

*E-mail address:* sthirumaran@yahoo.com (S. Thirumaran).

# Effect of co-crystallization of ethanol, pyridine and 2,2'-bipyridine on molecular aggregation in bis(1,2,3,4-tetrahydroquinolinedithiocarbamato-S,S')mercury(II) and synthesis of HgS nanoparticles

**Narayanaswamy Srinivasan[a], Subbiah Thirumaran*[a] and Samuele Ciattini[b]**

$[Hg(thqdtc)_2]$ (**1**) and $[Hg(thqdtc)_2(2,2'\text{-bipy})]$ (**2**) (where thqdtc = 1,2,3,4-tetrahydrquinolinecarbodithioate and 2,2'-bipy = 2,2'-bipyridine) have been prepared and characterized. Single crystal X-ray structural analysis show that $[Hg(thqdtc)_2] \cdot 0.5(2,2'\text{-bipy})$ (**3**), $[Hg(thqdtc)_2] \cdot 0.25C_2H_5OH$ (**4**) and $[Hg_3(thqdtc)_6] \cdot$ py (**5**) exist as monomer , dimer and trimer, respectively. Co-crystallization of 2,2'-bipyridine, ethanol and pyridine (py) with $[Hg(thqdtc)_2]$ causes a change in secondary interactions and hence, different structural motifs are obtained. Complexes **1** and **2** have been used as single source precursors for the preparation of HgS nanoparticles. The nanoparticles have been characterized by XRD, TEM, UV and fluorescence spectra. Use of **1** for the preparation of mercury sulfide afforded hexagonal shape HgS nanosheets and three different morphology HgS nanoparticles are obtained from **2**; most of the crystallites are rod while the remainders are hexagonal and rectangle sheets.

## Introduction

One of the areas in crystal engineering of greatest potential impact relates to the pharmaceutical industry – drug formulation and intellectual property- where issues relating to crystallization, polymorphism etc. are parameters. A focus of these crystal engineering studies relates to the preparation of multi-component crystals, often referred to as co-crystals, where, for example utilizing hydrogen bonding synthons, active pharmaceutical ingredients are co-crystallized with other molecules[1]. The idea of co-crystal formation is not restricted to applications in the

pharmaceutical industry alone but also finds in synthetic chemistry[2], in the generation of optical materials[3], even in epitaxial growth, where a crystal is grown upon another crystal. Five distinct structural motifs are reported for the mercury(II) bisdithiocarbamate complexes, $Hg(S_2CNR_2)$, ranging from mononuclear entities to dinuclear oligomers and two dimensional arrays[4]. There are two mononuclear motifs (motifs I and II). The central atom in motif I exists in a grossly distorted tetrahedral geometry[5-9] and motif II features a square planar geometry about the central atom[10-13]. Dinuclear motifs are formed that feature two chelating and two bridging dithiocarbamate ligands. The coordination geometry for mercury might be described as 4+1 [14] due to a weaker transannular Hg·····S interaction. Motifs III and IV exhibited difference in the inherent symmetry of dinuclear aggregate. In motif III, there is a centrosymmetric relationship implying that the bridging dithiocarbamate ligands are on either side of the central $Hg_2S_2$ trapezoidal plane whereas in motif IV, there is a two-fold symmetry so that bridging ligands are on the same side of the central plane. A larger structure (motif V) is found in only one complex ie., $[Hg(S_2CNH_2)_2]$[15]. All dithiocarbamate ligands are bridging and each mercury atom exists in a distorted tetrahedral geometry. The actual structure adopted in main group metal dithiocarbamate complexes is dependant of the organic functionality [16]. This general principle applies in the case of the structural chemistry of $[Hg(S_2CNR_2)_2]$ [4] , the vagaries of crystal packing considerations versus the dictates of flexible coordination geometries is , perplexingly, found for $Hg(S_2CNEt_2)$, where both mononuclear motif II [17,18] and dinuclear motif III [17,19] have been found. Nanoparticles of group II-VI chalcogenides, ME (M = Zn, Cd, Hg; E = S, Se, Te) have attracted an increasing interest during the recent years due to various areas of applications. Metal sulphide nanoparticles (MS) are useful material with wide application in many fields such as ultrasonic

transducers, image sensor, electrostatic image materials, flat-panel devices, photocatalysis, photoelectric conversion devices, non-linear optical material and solar cells [20-23].

Unexpectedly, ethanol, 2,2′-bipyridine and pyridine are co-crystallized with [Hg(thqdtc)$_2$] to form three different structural motifs. In this paper, we report the influence of co-crystallization of ethanol, 2,2′-bipyridine and pyridine on supramolecular aggregation in bis(1,2,3,4-tetrahydroquinolinedithiocarbamate)mercury(II). In addition, synthesis of HgS nanoparticles from [Hg(thqdtc)$_2$] and [Hg(thqdtc)$_2$(2,2′-bipy)] and their characterization are also presented.

## Results and Discussion

### Spectroscopy

The energy of the thioureide $\nu_{C-N}$ band is intermediate between the stretching frequencies associated with typical single and double bonded carbon and nitrogen atoms [24,25]. In the present study, [Hg(thqdtc)$_2$] and [Hg(thqdtc)$_2$(2,2′-bipy)] show the $\nu_{C-N}$(thioureide) at 1452 and 1454 cm$^{-1}$, respectively, indicating the partial double bond character. The $\nu_{C-S}$ bands appear at *ca*. 965 cm$^{-1}$ in both the complexes. The ring frequencies associated with 2,2′-bipyridine are observed in the range of 1600-1000 cm$^{-1}$ [26,27]. In the present study, 2,2′-bipyridine adduct shows a prominent band at 1581 cm$^{-1}$. The structures and numbering of thqdtc and 2,2′-bipy are given in Fig.1. In both the Hg(II) complexes, protons at C–2 and C–8 carbons undergo strong deshielding to give the signals around 4.26 and 7.20 ppm, respectively. A quintet observed around 2.05 ppm and a triplet observed around 2.80 ppm are due to the protons at C–3 and C–4. A multiplet is expected for protons at C–5, C–6 and C–7 of thqdtc. But a triplet observed around 7.93 ppm is due to

overlapping of signals of protons at C–5, C–6 and C–7 of thqdtc. Apart from these signals, four signals appear in the downfield region of 7.34 to 8.70 ppm which are due to ring protons of 2,2′-bipyridine for [Hg(thqdtc)$_2$(2,2′-bipy)].

Free 1,2,3,4-tetrahydroquinoline shows signals at 41.9 ppm due to C–2 carbon. In the case of [Hg(thqdtc)$_2$] and its 2,2′-bipyridine adduct, the C–2 carbon of thqdtc gets deshielded and gives signal around 55.0 ppm. The downfield shift of C–2 carbon signal in the case of the complexes is due to reduction in the electron density in their vicinity, which contribute to a significant thioureide structure $N^{\delta+}$⋯$C^{\delta-}$ in the complexes. The most important $^{13}$C NMR signals of the $N^{13}CS_2$ carbons are observed at 205.4 and 205.8 ppm for [Hg(thqdtc)$_2$] and [Hg(thqdtc)$_2$(2,2′-bipy)], respectively with very weak intensity characteristic of the quaternary carbon signals. In the Na(thqdtc).2H$_2$O, the $NCS_2$ carbon resonance appeared at 212.6 ppm, which then shifted upfield in the complexes by ~7 ppm. The upfield shift in the $NCS_2$ carbon signal is an indication of deshielding of this carbon upon complexation of the ligand to $Hg^{2+}$. In both the complexes, the aromatic carbon signals are observed at 121.0-155.9 ppm.

**Structural analysis**

In the case of **1** and **2**, suitable crystals for single crystal X-ray analysis were not obtained. Recrystallization of **1** and **2** in various solvents yielded crystals of **3**, **4** and **5**. Single crystal X-ray analysis of **3**, **4** and **5** were carried out.

**Monomeric [Hg(thqdtc)$_2$] · 0.5(2,2′-bipy) (3).** ORTEP of **3** is shown in Fig. 2. Complex **3** crystallized in the triclinic space group P-1 which contains two molecules per unit cell. Half a molecule of 2,2′-bipyridine is co-crystallized along with the complex molecule. $Hg^{2+}$ is coordinated by four sulphur atoms from two chelating dithiocarbamates. Dihedral angle of the two chelate planes Zn-S-C-S in **3** is 81.53°. This indicates that the coordination geometry around the mercury atom is a distorted tetrahedral arrangement of four sulphur atoms. The geometry adopted by this complex is similar to the motif I. In **3**, there are considerable differences between the pairs of Hg–S and S–C bonds and it is interesting to note that the shorter Hg–S bonds [2.3510(15), 2.3636(15) Å compared to 2.9930(15), 2.9606(15) Å] are associated with the longer S–C distances [1.745(5), 1.752(5) Å *versus* 1.691(6), 1.701(5) Å]. The fact is that the dithiocarbamate ligand is asymmetrically linked to mercury and the asymmetric C–S distances are shorter than the typical C–S single bond distance (1.81 Å). Therefore all the C–S bonds in the present structure are of partial double bond character as observed in most of the dithiocarbamates [5-7].

The short thioureide C–N distance, 1.337(7) Å indicates that the π-electron density is delocalized over the $S_2CN$ moiety and that this bond has a significant double bond character. A close inspection of the crystal structure indicates that the structure of **3** reveals a tendency for molecular aggregation. As shown in Fig. 3 for the structure of **3** molecules are oriented to allow for the formation of intermolecular Hg···S interactions [Hg···S1 = 3.554(1) Å and Hg···S4 = 3.444(2) Å]. But these are not indicative of significant bonding interactions [28].

**Dimeric [Hg(thqdtc)$_2$] · 0.25$C_2H_5OH$ (4)**. ORTEP of **4** is shown in Fig. 4. Four units of [Hg(thqdtc)$_2$] · 0.25$C_2H_5OH$ are present in the unit cell. 0.25 Molecule of ethanol is co-

crystallized along with the complex molecule and are disordered. One molecule of ethanol is co-crystallized per unit cell. $Hg^{2+}$ ion is coordinated to four sulphur atoms from the dithiocarbamates. In **4**, there are considerable differences between the pairs of Hg–S bonds [2.396(3), 2.365(3) Å compared to 2.757(3), 2.953(4) Å]. There is an apparent tendency for the related S–C distances also to show asymmetry [1.747(11), 1.752(11) Å *versus* 1.695(10), 1.702(11) Å]. This indicates that the dithiocarbamate ligand is asymmetrically linked to mercury. The mercury atom exists in an $S_4$ donor set that defines a highly distorted tetrahedral geometry with a range of angles from 66.82(9)º, *i.e.,* the chelate angle, to 163.88(12)º, *i.e.,* involving the more strongly bound S4 and S2 atoms. Two molecules associate in the crystal structure by weak Hg–S ($Hg1–S1^i = Hg1^i–S1$ = 3.200(2) Å) bonds (symmetry code: i = 1–x, 1–y, 1–z). This distance, while long, is within the sum of the van der Waals radii of the atoms [31]. If the long $Hg–S1^i$ bond is considered, the coordination geometry adopted by this complex is intermediate between tetragonal pyramid (TP) and trigonal bipyramid (TBP) (motif III; $\tau_5$ = 0.64). Two molecules associate as shown in Fig. 5. Additional stabilization to the dimer is afforded by C(12)—H(12B)···S(4) (H12···S4 = 2.912(3) and C12···S4 = 3.617(4) Å). Average C–N bond distance is 1.336(12) Å which clearly indicates the contribution of the thioureide form to the dithiocarbamate ligand. This contrasts well with adjacent typical single bonded N–C distance [mean = 1.467(13) Å].

**Trimeric $[Hg_3(thqdtc)_6]$ · py (5).** ORTEP of **5** is shown in Fig.6. The single crystal X-ray structure of **5** contains one molecule per unit cell. one molecule of py is co-crystallized along with the complex molecule. The environments of $Hg^{2+}$ ions Hg1 and $Hg1^i$ (symmetry code: i = 1–x, 1–y, –z) in $[Hg_3(thqdtc)_6]$ · py are similar but their environments are different from that of Hg2. Hg1 atom coordinates to four sulphur atoms (S1, S2, S3, S4) at distances of 2.394-2.927 Å and a

fifth sulphur atom (S6) at 3.052 Å. The geometry of the coordination polyhedron [$HgS_5$] is intermediate between tetragonal pyramid (TP) and trigonal bipyramid (TBP) ($\tau_5$ = 0.64) [29]. Hg2 lies on an inversion centre and is coordinated by a pair of dithiocarbamate ligand (S5, S6, $S5^i$, $S6^i$). There are two short Hg–S bond distances of 2.3678(15) Å and two longer Hg–S contacts of 2.9535(18) Å which have been elongated due to the sharing of the relevant sulphur atoms with the adjacent mercury atoms Hg1 and $Hg1^i$. Because of the small bite angle associated with the dithiocarbamate moiety [S5–Hg2–S6 = 67.27(5)°], the Hg2 is in a highly distorted square planar coordination environment.

All the C–S bond lengths [mean = 1.721(7) Å] lie approximately between values expected for single and double bonds *i.e.,* 1.81 Å and 1.61 Å[30], respectively and thus have a considerable double bond character. The C–N bond length of 1.319(7) Å indicates that this bond also has significant double bond character[5-7].

**Comparative structural analysis.** Single crystal X-ray structural analysis show that [$Hg(thqdtc)_2$] · 0.5(2,2′-bipy), [$Hg(thqdtc)_2$] · 0.25$C_2H_5OH$ and [$Hg_3(thqdtc)_6$] · py exist as monomer, dimer and trimer, respectively. Comparative structural parameters are given in Table 1. The interatomic parameters related to mercury atom geometries in [$Hg(thqdtc)_2$] · 0.5(2,2′-bipy), [$Hg(thqdtc)_2$] · 0.25$C_2H_5OH$ and [$Hg_3(thqdtc)_6$] · py exhibit two interesting trends. Firstly, it must be noted that there are significant disparities in the Hg–S bond distances, *i.e.,* for a particular dithiocarbamate ligand one Hg–S bond distance is significantly shorter than the other. Further, the presence of S–Hg–S angle *ca.* 165°, *i.e.,* involving the more strongly bound S atoms, is wider than the ideal 90° (square planar geometry) or 109.5° (tetrahedral geometry) angles. The two short Hg-S distance in **3-5** indicate that the valency at mercury

should be satisfied by two covalent Hg–S interactions. This also shows that the valency of mercury in all the complexes **1**-**5** is 2. The presence of more than two Hg–S bonds are weak Hg···S interactions. These are weaker than conventional covalent bond and termed secondary interactions. Given the geometry data cited above, it is possible to conclude that the molecular structures may be recorded as being comprised of linear S–Hg–S groups in accord with the conventional valence shell electron pair repulsion model as represented in scheme 1, distortions not withstanding. Additional Hg···S interactions occur to give rise to differing molecular aggregates. Co-crystallization of 2,2′-bipy, $C_2H_5OH$ and py with $[Hg(thqdtc)_2]$ causes a change in secondary interactions. Hence, different structural motifs are obtained.

**Characterization of mercury sulphide nanoparticles**

To study the crystalline structures of the products, PXRD measurements were carried at room temperature. The HgS nanoparticles synthesized from $[Hg(thqdtc)_2]$ and $[Hg(thqdtc)_2(2,2'\text{-bipy})]$ are represented as HgS**1** and HgS**2**, respectively. The powder X-ray diffraction patterns of the HgS**1** and HgS**2** are shown in Fig. 7. All the diffraction peaks could be indexed to be a pure hexagonal phase HgS (cinnabar). In the XRD pattern, no peaks of any impurities were detected, indicating the high purity of the product. The unit cell parameters were accurately calculated *via* rietveld fit using le bail method. The rietveld plots of prepared mercury sulphides are shown in Fig. 8 and the unit cell values are given in Table 2. The calculated lattice parameters are in good agreement with the literature values (JCPDS Card no. 6-0256).

The dimensions and morphologies of the products were observed by TEM measurements. TEM analysis for HgS**1** and HgS**2** nanoparticles are shown in Fig. 9. The results of the TEM studies are

summarized in Table 3. TEM micrographs show that the HgS**1** nanoparticles are hexagonal sheets. Three types of morphologies are present in HgS**2**; most of the crystallites are rod while the remainder are hexagonal and rectangle sheets. The diameter of the nanorods is in the range 30-56 nm and the length is in the range 285-450 nm. As shown in Fig. 9 (HgS**2**), nanorods are assembled to parallel to each other. The thickness of all the synthesized hexagonal sheets is *ca*. 5 nm and the length is in the range 74-1300 nm. Only one type of morphology (hexagonal sheets) is observed in the case of HgS**1**. But three different shapes are observed in the case of HgS**2**. This indicates that the presence of nitrogen donor ligand (2,2'bipy) in **2** affects the shapes of the HgS nanoparticles.

UV-vis absorption spectra of HgS1 and HgS2 are shown in Fig. 10. An absorption band was observed at 275nm for HgS1 and HgS2 nanoparticles. The clear appearance of a blue–shift of the absorption peaks relative to bulk HgS (620nm) [31] indicates that the HgS nanoparticles are quantum-confined.

Fluorescence spectra of HgS1 and HgS2 are shown in Fig. 11. The fluorescence spectra of HgS1 and HgS2 exhibit two emission peaks through the excitation at 460nm. One is the sharp emission peak at 540 nm and the other is a broad red emission peak around 630 nm. The emission peak around 540 nm is attributed to the core-state radioactive decay from CB to VB and the emission peak blue shifts due to quantum-confined effect (bulk HgS: 588nm)[32]. The additional broad red emission in fluorescence spectra at 630 nm is attributed to the combination of trapped electrons/holes in some surface defect states of HgS particles.

## Conclusions

Compounds **1** and **2** were prepared and studied by means of IR and NMR ($^{1}H$ and $^{13}C$) spectroscopy. The structures of the $[Hg(thqdtc)_2] \cdot 0.5(2,2'\text{-bipy})$ (**3**), $[Hg(thqdtc)_2] \cdot$

$0.25C_2H_5OH$ (**4**) and $[Hg_3(thqdtc)_6] \cdot py$ (**5**) suggest that molecular aggregation can be modified by co-crystallization of various molecules with mercury dithiocarbamate complexes and different structural motifs can be obtained. Only one type of morphology (hexagonal) is observed in the HgS nanosheets prepared from **1** and three different morphologies are observed in the HgS nanoparticles prepared from **2**. This indicates that the presence of nitrogen donor ligand (2,2'-bipy) in **2** affects the shapes of the HgS nanoparticles.

## Experimental

**Synthesis and Characterization.** 1,2,3,4-Tetrahydroquinoline (Alfa Aesor), carbon disulfide and mercury chloride (Merck), 2,2′-bipyridine (Himedia) and ethylenediamine (Merck) were used as supplied. IR spectra were recorded on a Thermo Nicolet Avatar 330 FT-IR spectrophotometer (range; 400–4000 $cm^{-1}$) as KBr pellets. The NMR spectra were recorded on JEOL GS × 400 spectrometer operating at 400 MHz. A Shimadzu UV-1650 PC double beam UV-Visible spectrophotometer was used for recording the electronic spectra. The spectra were recorded in chloroform and the pure solvent was used as the reference. Fluorescence measurements were made using a Jasco FP-550 spectrofluorimeter.

**Preparation of 1.** An aqueous solution of $HgCl_2$ (10 mmol, 2.7 g) was added drop wise to an aqueous solution of $Na(thqdtc) \cdot 2H_2O$ (20 mmol, 5.34 g) at ice cold temperature. The reaction mixture was stirred for 1 h and the precipitate was filtered. The product was washed several times with cold water and then dried[33]. IR (KBr, $cm^{-1}$): 1452 ($\nu_{C-N}$), 963 ($\nu_{C-S}$); $^1H$ NMR ($CDCl_3$, ppm): 4.27(t, H–2), 2.05(quintet, H–3), 2.81 (t, H–4), 7.92(t, H–5, H–6 and H–7), 7.16–7.26 (m, H–8) (aromatic protons); $^{13}C$ NMR ($CDCl_3$, ppm): 55.3 (C–2), 26.2 (C–3), 24.0

(C–4), 125.7, 126.2, 127.4 and 128.2 (C–5, C–6, C–7 and C–8), 133.5 (C–4a), 141.2 (C–8a) (aromatic carbons), 205.4 ($NCS_2$).

**Preparation of 2.** A hot solution of 2,2'-bipyridine (2 mmol, 0.31 g) in ethanol was added to a hot solution of [Hg(thqdtc)$_2$] (1 mmol, 0.62 g) in chloroform. The resulting yellow solution was cooled and then added with petroleum ether (boiling range: 40-60°C). Yellow precipitate of the adduct separated out, which was filtered and dried. Yield: 78%; m.p. 196°C; *Anal. Found (Calc.)*: C, 46.3 (46.6); H, 3.7 (3.6); N, 7.1 (7.2%). IR (KBr, $cm^{-1}$): 1454 ($\nu_{C-N}$), 965 ($\nu_{C-S}$); $^1$H NMR ($CDCl_3$, ppm): 4.26(t, H–2), 2.11(quintet, H–3), 2.78(t, H–4), 7.93(t, H–5, H–6 and H–7), 7.17–7.21 (m, H–8) (aromatic protons), 8.70 [d, H–3 (bipy)], 7.34 [t, H–4 (bipy)], 7.84 [t, H–5 (bipy)], 8.42 [d, H–6 (bipy)]; $^{13}$C NMR ($CDCl_3$, ppm): 55.0 (C–2), 26.1 (C–3), 23.9 (C–4), 125.6, 126.1, 127.1 and 128.1 (C–5, C–6, C–7 and C–8), 133.3 (C–4a), 141.2 (C–8a) (aromatic carbons), 205.8 ($NCS_2$), 155.9 (C–1, bipy), 149.0 (C–3, bipy), 123.6 (C–4, bipy), 136.8 (C–5, bipy), 121.0 (C–6, bipy).

**Preparation of 3.** [Hg(thqdtc)$_2$(2,2′-bipy)] (**2**) (0.7g) was dissolved in hot benzene-chloroform solvent mixture (1:1, 60 ml). The yellow solution obtained was filtered and left for evaporation at room temperature. After four days, pale yellow crystals of **3** separated out, which was filtered. Yield: 46%; m.p. 190 °C; Anal. for **3**: *Found (Calc.)*: C, 42.7 (43.2); H, 3.3 (3.5); N, 5.8 (6.0%) IR (KBr, $cm^{-1}$):1455 ($\nu_{C-N}$), 966 ($\nu_{C-S}$).

**Preparation of 4.** [Hg(thqdtc)$_2$] (**1**) (0.6g) was dissolved in hot ethanol-water solvent mixture (10:1, 50 ml). The pale yellow solution obtained was filtered and left for evaporation at room temperature. After five days, pale yellow crystals of **4** separated out, which was filtered. Yield:

38%; m.p. 160 °C; Anal. for **4**: *Found (Calc.)*: C, 38.6 (39.2); H, 3.4 (3.4); N, 4.4 (4.5%); IR (KBr, $cm^{-1}$): 1448 ($\nu_{C-N}$), 967 ($\nu_{C-S}$).

**Preparation of 5.** $[Hg(thqdtc)_2]$ (**1**) (0.6g) was dissolved in 50 ml of warm pyridine. . The yellow solution obtained was filtered and kept for evaporation at room temperature. After 25 days, pale yellow crystals of **5** separated out, which was filtered. Yield: 51%; m.p. 152 °C; Anal. For **5**: *Found (Calc.)*: C, 40.0 (40.4); H, 3.3 (3.4); N, 4.9 (5.1%) IR (KBr, $cm^{-1}$): 1445 ($\nu_{C-N}$), 966 ($\nu_{C-S}$).

**Preparation of HgS Nanoparticles.** 0.5 g of $[Hg(thqdtc)_2]$ was dissolved in 15 mL of ethylenediamine in a flask and then heated to reflux (117°C) and maintained at this temperature for 2 min. The red precipitate obtained was filtered off and washed with ethanol. Similar procedure was adopted for the preparation of HgS nanoparticles from $[Hg(thqdtc)_2(2,2'\text{-bipy})]$ (scheme 2).

**X-Ray Crystallography**

Details of the crystal data and structure refinement parameters are summarized in Table 4. The intensity data for $[Hg(thqdtc)_2] \cdot 0.5(2,2'\text{-bipy})$, $[Hg(thqdtc)_2] \cdot 0.25\ C_2H_5OH$ and $[Hg_3(thqdtc)_6] \cdot$ py were collected at ambient temperature (293(2) K) on Oxford Diffraction Xcalibur 3 (with CCD) diffractometer using graphite monochromated MoK$\alpha$ radiation ($\lambda$ = 0.71073 Å and $\lambda$ = 0.71069 Å). The structures of $[Hg(thqdtc)_2] \cdot 0.5(2,2'\text{-bipy})$, $[Hg(thqdtc)_2] \cdot 0.25\ C_2H_5OH$ and $[Hg_3(thqdtc)_6] \cdot$ py are solved by SHELXS-97[34] and refined by full matrix least square with SHELXL-97[35]. Pyridine molecule in complex **4** is modeled as disordered across a symmetry element, with EXYZ constrained carbon and nitrogen atoms (C32 and N4) sharing one site. The occupancy was constrained by symmetry to be 0.5. Selecteted bond distances and angles are

shown in Table 5. Crystallographic data have been deposited with the Cambridge Crystallographic Centre as supplementary publications numbers CCDC-740716, 740717 and 740714 for $[Hg(thqdtc)_2] \cdot 0.5(2,2'\text{-bipy})$, $[Hg(thqdtc)_2] \cdot 0.25\ C_2H_5OH$ and $[Hg_3(thqdtc)_6] \cdot py$, respectively. Copies of the data can be obtained free of charge on application to CCDC, 12 Union Road, Cambridge CBZ 1EZ, UK.

**Notes and References**

[a] *Department of Chemistry, Annamalai University, Annamalinagar 608 002, Tamilnadu, India*
[b] *Centro di Cristallografia Strutturale, Polo Scientifio di Sesto Fiorentino, Via della Lastruccia N°3, 50019 Sesto Fiorentino, Firenze, Italy*

* Corresponding author. Tel.: +91 9842897597.

*E-mail address:* sthirumaran@yahoo.com (S. Thirumaran).

1 P. Vishweshwar, J.A. McMahon, J.A. Bis, M.J. Zaworotko, J. Pharm. Sci., 2006, **95**, 499–516.

2 T. Friscic, L. R. MacGillivray, *Chem. Commun*. 2005, 5748–5750.

3 T. Friscic, L. R. MacGillivray, *Z. Kristallogr*., 2005, **220**, 351–363.

4 C. S. Lai, E. R. T. Tiekink, *CrystEngComm.,* 2003, **5**, 253-261.

5 C.S. Lai, E.R.T. Tiekink, *Appl. Organomet. Chem.,* 2003, **17**, 143-143.

6 M. Ito, H. Iwasaki, *Acta Crystallogr. B,* 1979, **35**, 2720-2721.

7 M.J. Cox , E.R.T. Tiekink, *Z. Kristallogr.,* 1999, **214**, 571-579.

8 M.J. Cox , E.R.T. Tiekink, *Main Group Met. Chem.,* 2000, **23**, 793-794.

9 C.S. Lai, E.R.T. Tiekink, *Appl. Organomet. Chem.,* 2004, **18,** 104-104.

10 M.J. Cox, E.R.T. Tiekink, *Z. Kristallogr.,* 1997, **212**, 542-554.

11 H. Iwasaki, *Acta Crystallogr. B,* 1973, **29**, 2115-2124.

12 P.C. Healy, A.H. White, *J. Chem. Soc., Dalton Trans.,* 1973, 284-287.

13 R. Alan Howie, E.R.T. Tiekink, J.L. Wardell, S.M.S.V. Wardell, *J. Chem. Crystallogr.,* 2009, **39**, 293-298.

14 I.Haiduc, F. T. Edelmann, Supramolecular Organometallic Chemistry Wiley–VCH, Weinheim, 1999.

15 C. Chieh, S.K. Cheung, *Can. J. Chem*., 1981, **59,** 2746-2749.

16 M.J. Cox, E.R.T. Tiekink, Rev. Inorg. Chem., 1997, 17, 1

17 H. Iwasaki, *Acta Cryst.* 1973, **B29**, 2115-2124.

18 P. C. Healy, A. H. White, *J. Chem. Soc., Dalton Trans.*, 1973, 284-287.

19 C.S. Lai, E.R.T. Tiekink, *Z. Kristallogr.-New Cryst. Struct.,* 2002, **217**, 593-94.

20 N. Tokyo, *Jpn. Kokai Pat.* 75130378 (C1.H01L.C01B), 1975.

21 N. Tokyo, K. Azkio, *Jpn. Kokai Pat.* 7855478 (C1.C23C15/00), 1978.

22 N. Tokyo, *J. Appl. Phys.,* 1975, **46**, 4857-4861.

23 Y. Li, X. Li, C. Yang, Y. Li, *J. Mater. Chem.,* 2003, **13**, 2641-2648.

24 L. Ronconi, L. Giovagnini, C. Marzano, F.B. Effio, R. Graziani, G. Pilloni, D. Fregona, *Inorg. Chem.,* 2005, **44**, 1867-1881.

25 R. Baggio, A. Frigerio, E.B. Halac, D. Vega, M. Perec, *J. Chem. Soc., Dalton Trans.,* 1992, 549-554.

26 B. Martin, W.R. McWhinnie, G.M. Waind, *J. Inorg. Nucl. Chem.,* 1961, **23**, 207-223.

27 S.P. Sinha, *Spectrochim. Acta,* 1964, **20**, 879-886.

28 A. Bondi, *J. Phys. Chem.,* 1964, **68**, 441-451.

29 A.W. Addison, T.N. Rao, J. Reedijk, J.V. Rin, G.C. Verschoor, *J. Chem. Soc., Dalton Trans.,* 1984, **7**, 1349-1356.

30 L. Pauling, The Nature of Chemical Bond, 3rd edn., Cornell Ithaca, New York, 1960.

31 A.J. Canty, G.B. Deacon, *Inorg. Chim. Acta*, 1980, **45**, L225-L227.

32 A.R.Rao, V. Dutta, V. N. Singh, *Adv.Matr.,* 2008, **20**, 1945-1951.

33 B.S. Garg, R.K. Garg, M.J. Reddy, *Indian J. Chem. A,* 1993, **32**, 697-700.

34 G.M. Sheldrick, *Acta Crystallogr.,* 1990, **46**, 467-473.

35 G.M. Sheldrick, SHELXL-97, University of Gottingen, Gottingen, Germany, 1997.

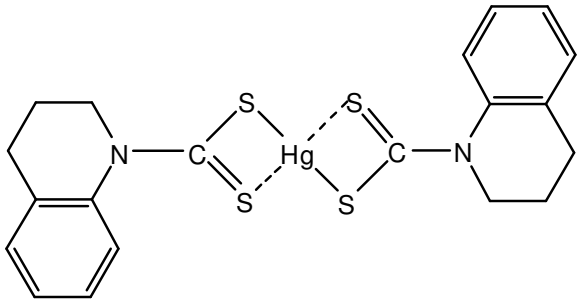

**Scheme 1** Chemical structure for [Hg(thqdtc)$_2$] pertaining to Figs**. 2**, **4** and **6**.

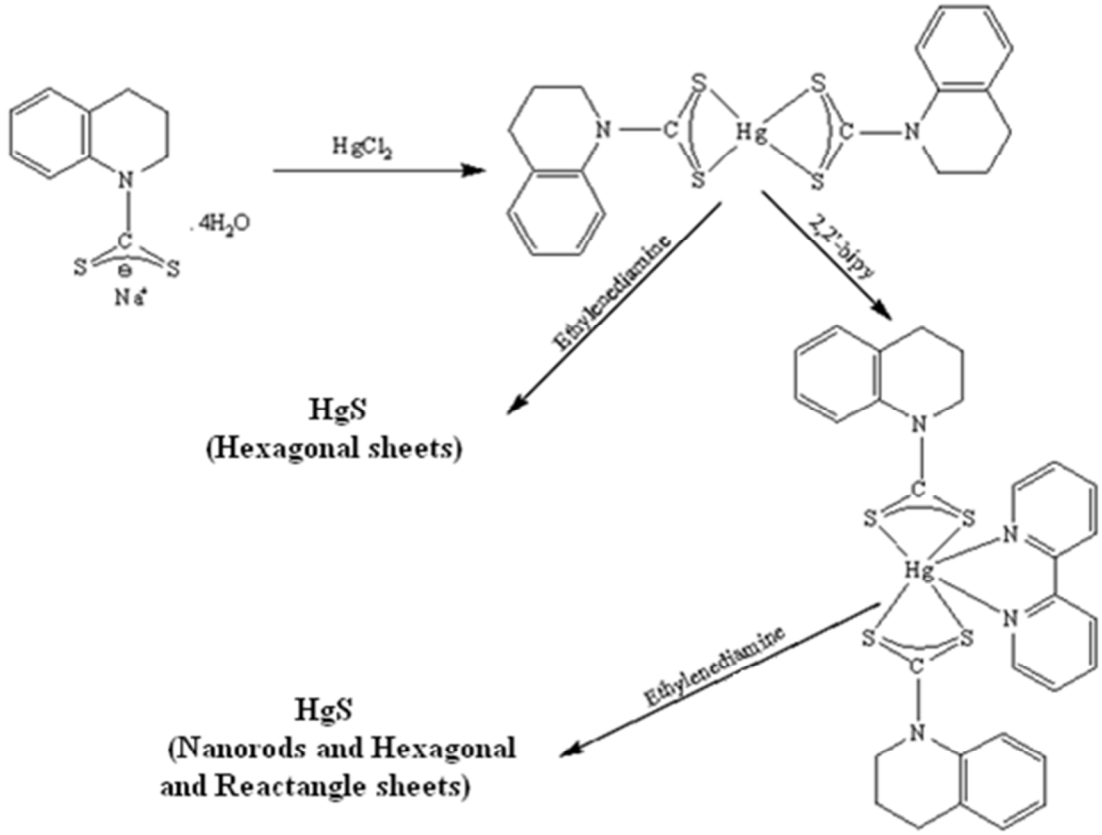


**Scheme 2** Schematic illustration for the preparation of HgS nanoparticles

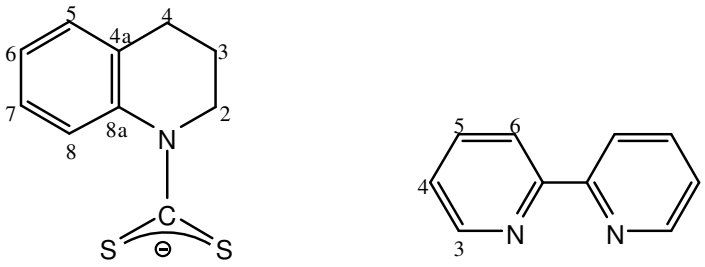


**Fig. 1** The structures and numbering of thqdtc and 2,2′-bipy.

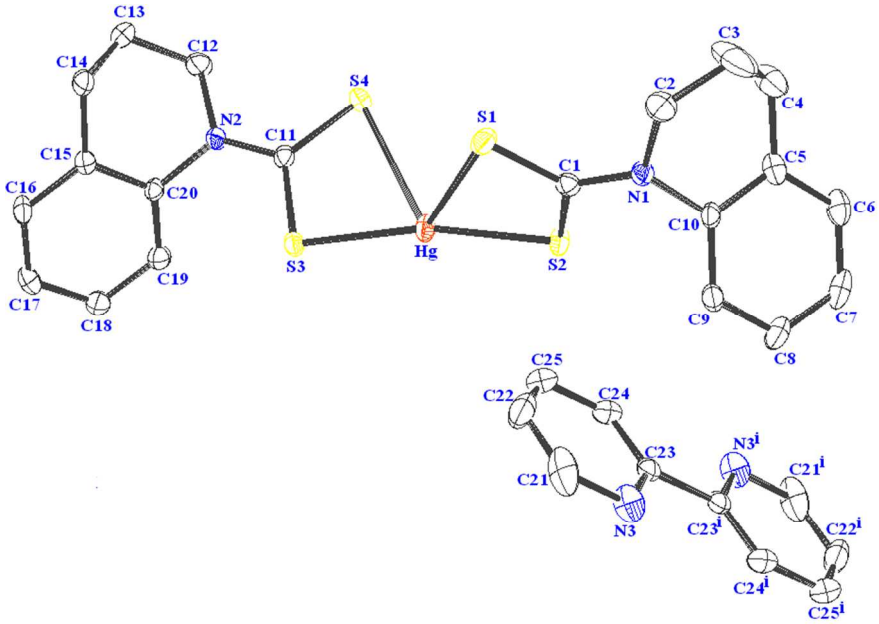


**Fig. 2** ORTEP diagram of [Hg(thqdtc)$_2$] · 0.5(2,2′-bipy) (**3**) . (symmetry code: i = 1–x, –y, 1–z).

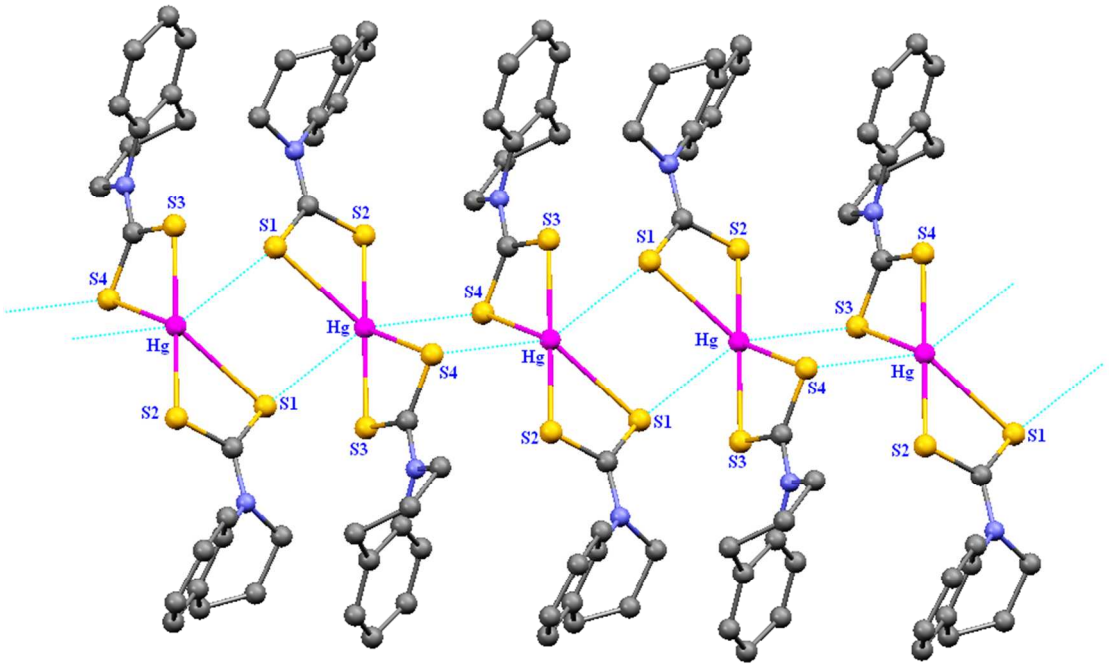


**Fig. 3** Molecular aggregation via intermolecular interaction in the crystal structure of [Hg(thqdtc)$_2$] · 0.5(2,2′-bipy) showing the potential of the monomeric motif to polymerize.

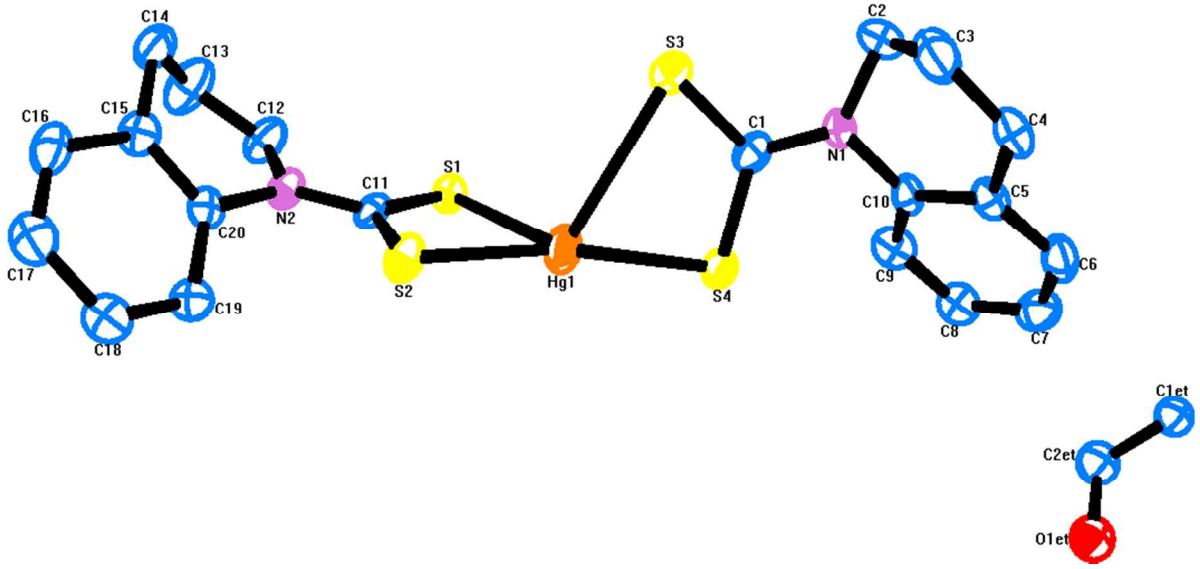


Fig. **4** ORTEP diagram of [Hg(thqdtc)$_2$] · 0.25 $C_2H_5OH$ (**4**).

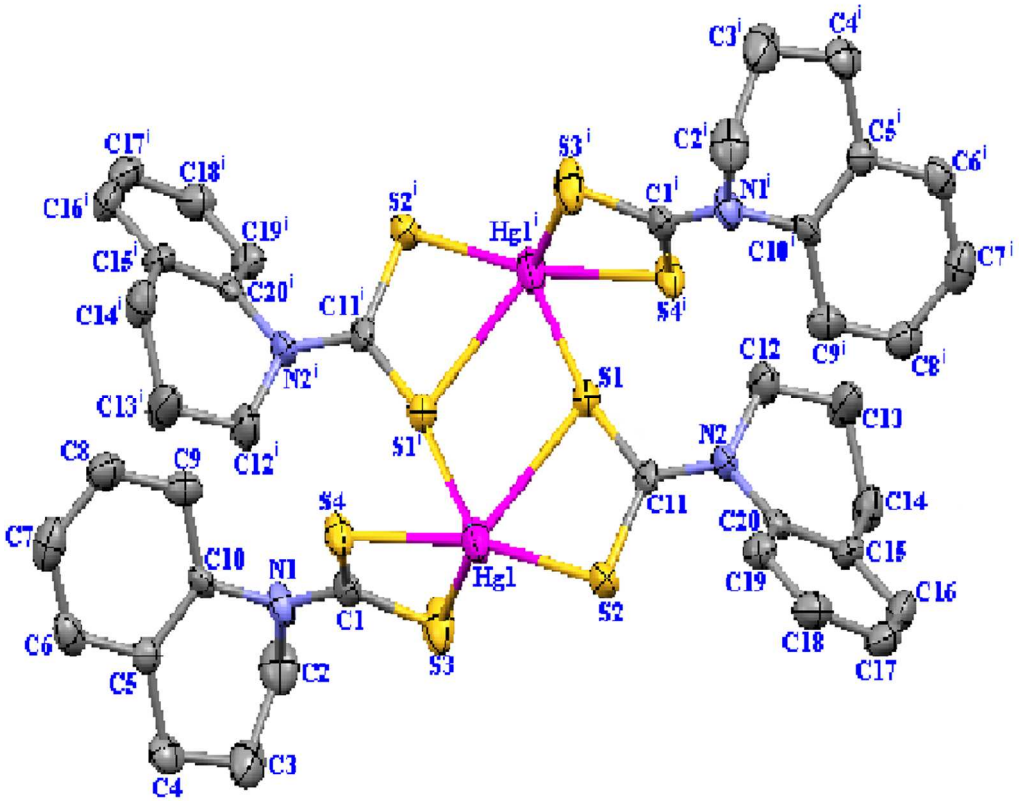


**Fig. 5** Dimeric structure of **4** (symmetry code: i = 1–x, 1–y, 1–z).

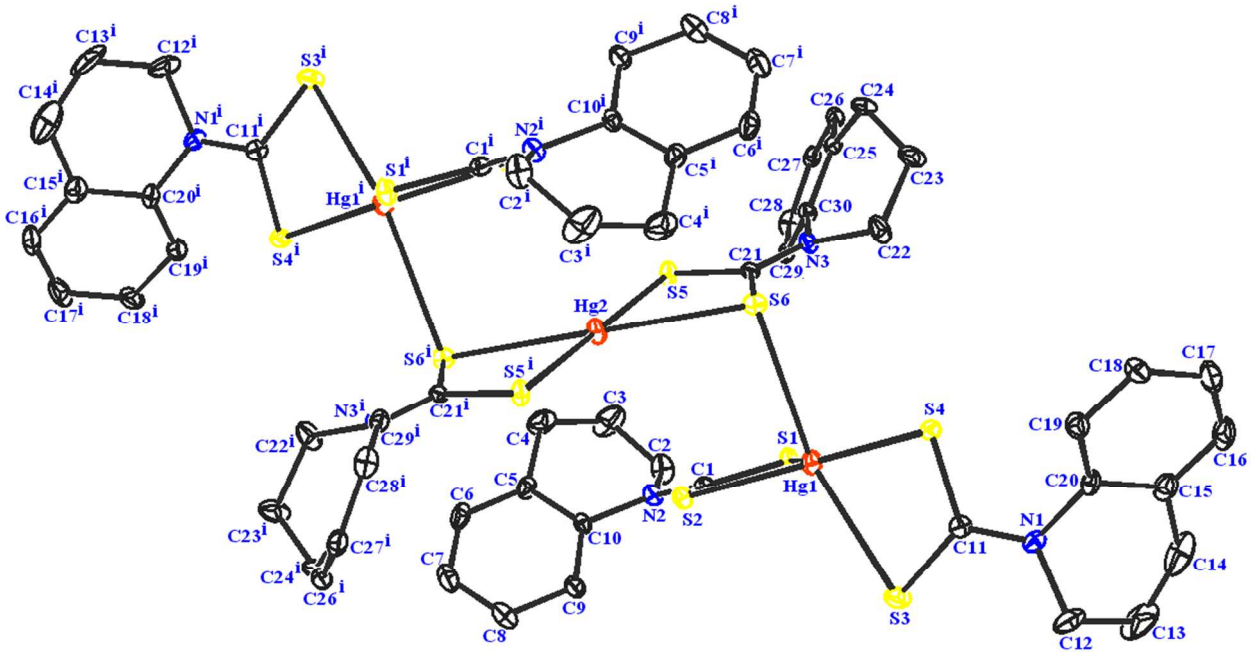


**Fig. 6** ORTEP diagram of $[Hg_3(thqdtc)_6] \cdot py$ (**5**) (hydrogen atoms have been omitted for clarity; symmetry code: i = 1–x, 1–y, –z).

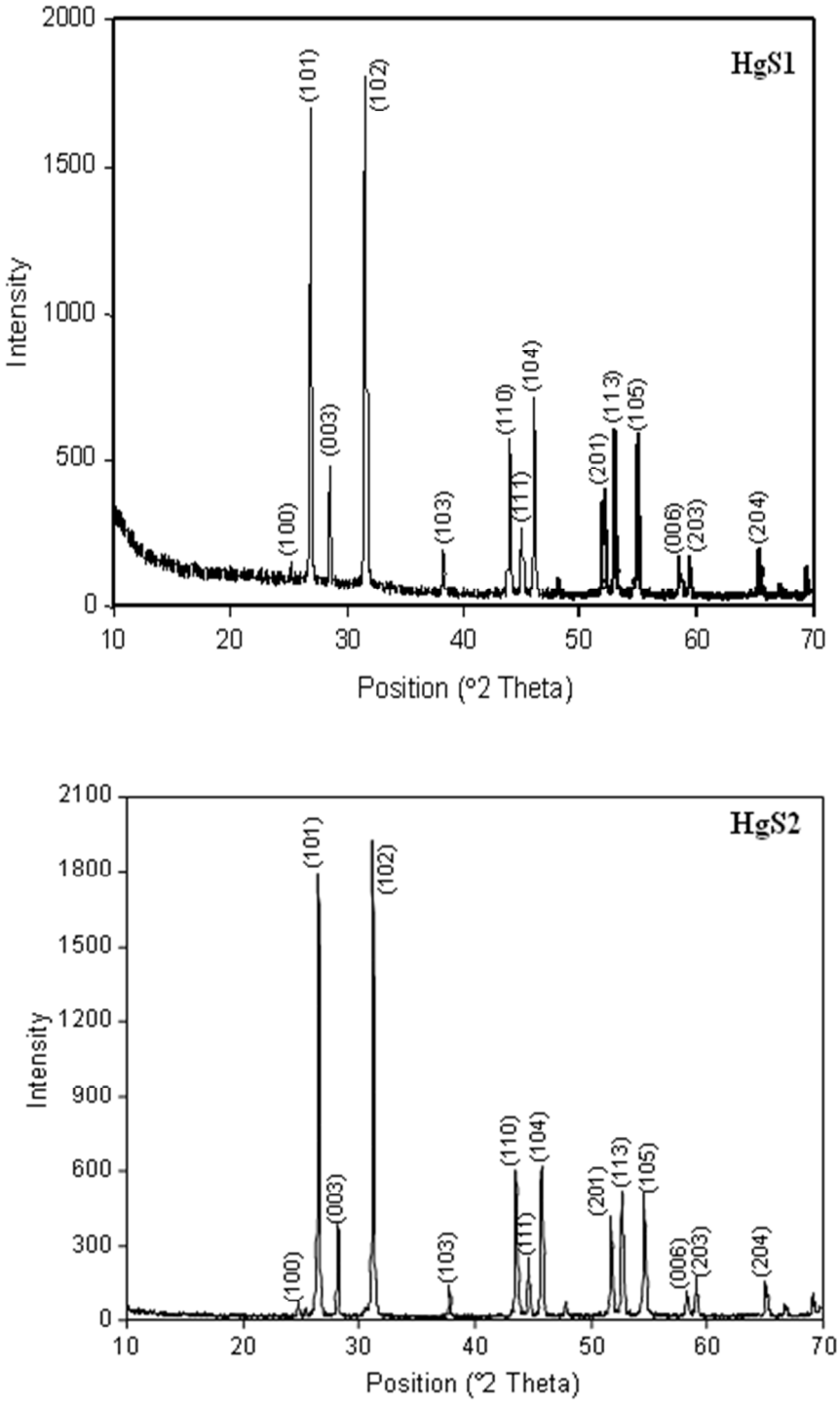


**Fig. 7** Powder X-ray diffraction patterns of HgS**1** and HgS**2**nanoparticles.

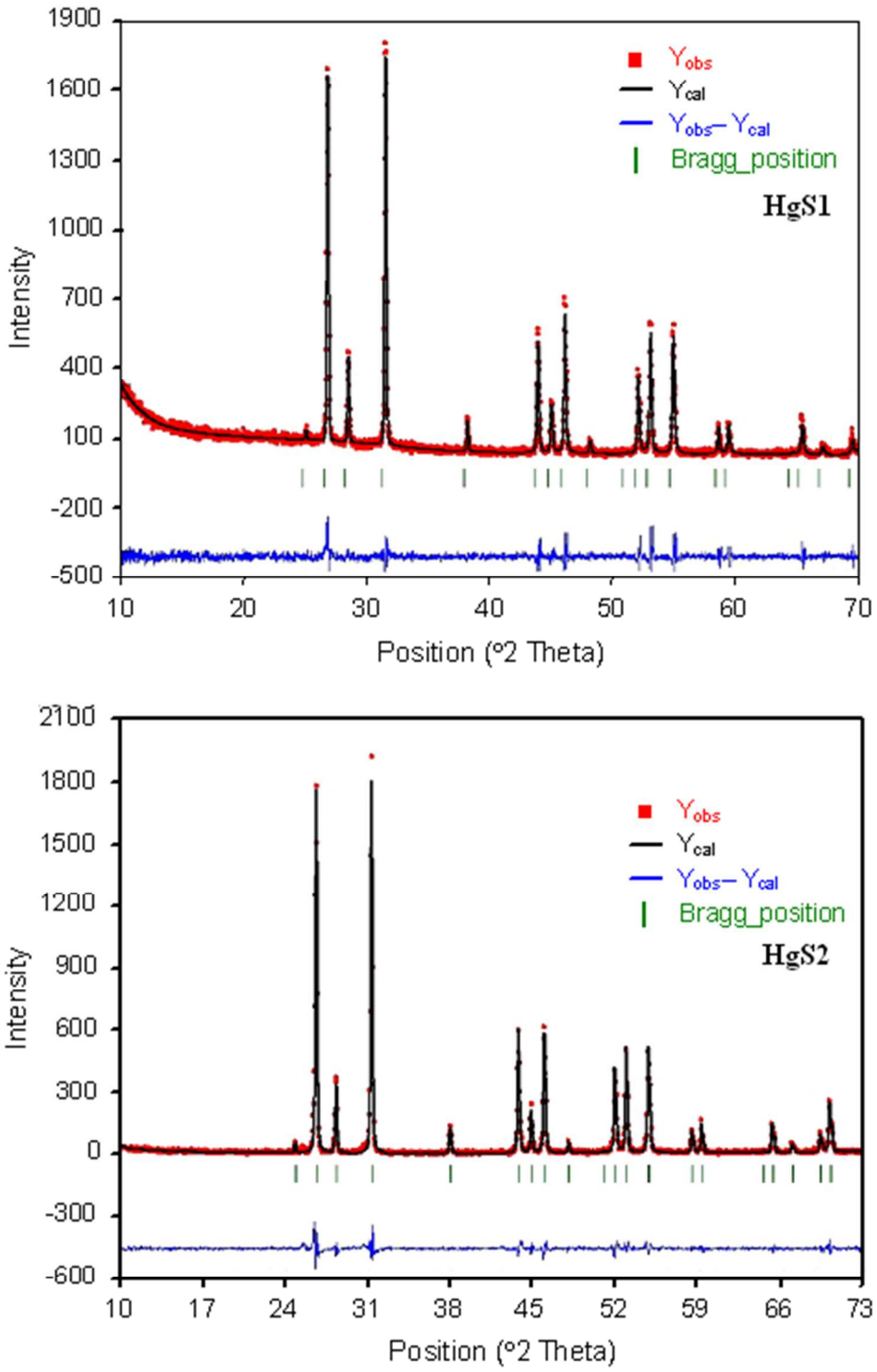


**Fig. 8** Rietveld plots of the HgS**1** and HgS**2** nanoparticles show the observed data as dots, calculated model fit as continuous line and residual in the bottom. The Bragg peaks also marked as bars.

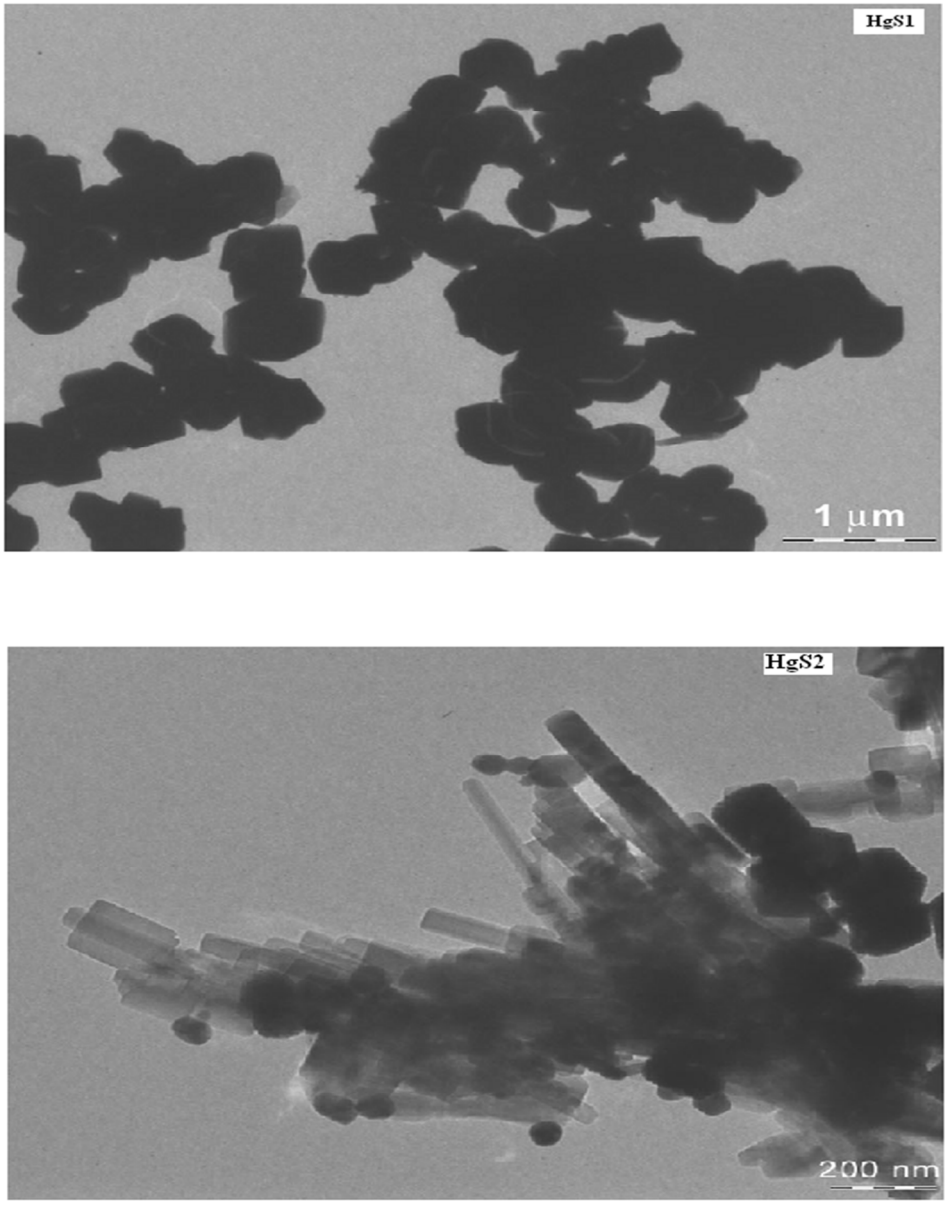


**Fig. 9** TEM images of HgS**1** and HgS**2**.

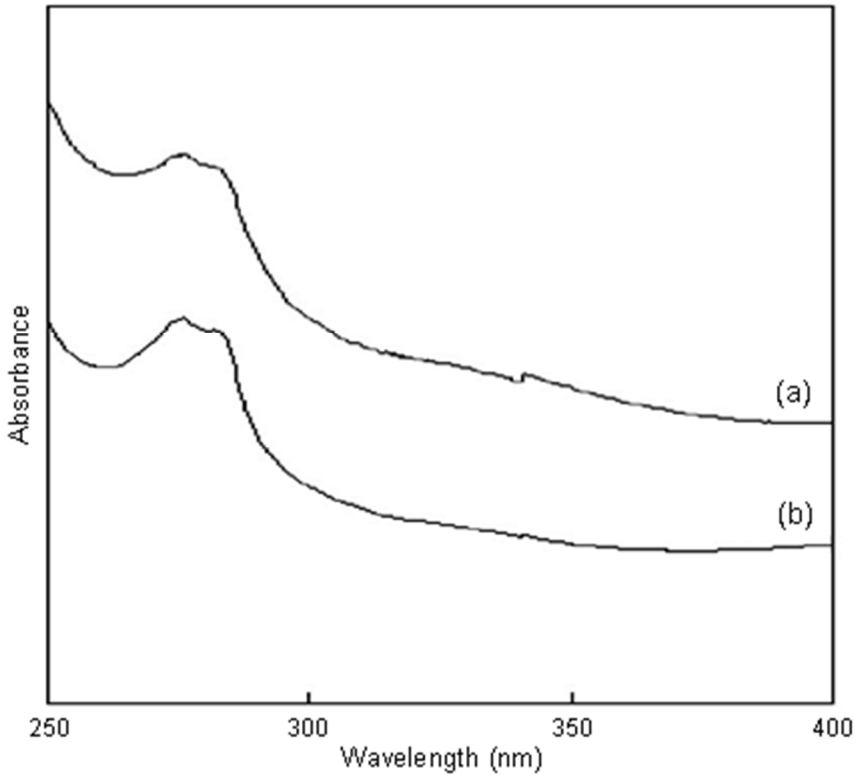


**Fig. 10** UV-Vis spectra of (a) HgS**1** and (b) HgS**2**

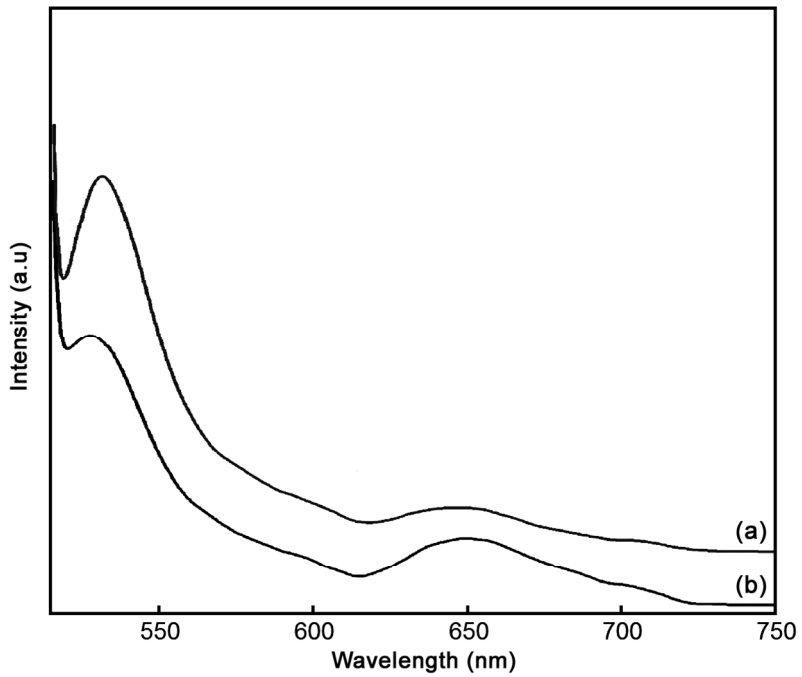


**Fig. 11** Fluorescence spectra of (a) HgS**1** and (b) HgS**2**

Different structural motifs are obtained by co-crystallization of 2,2'-bipyridine, ethanol and pyridine with $[Hg(thqdtc)_2]$.

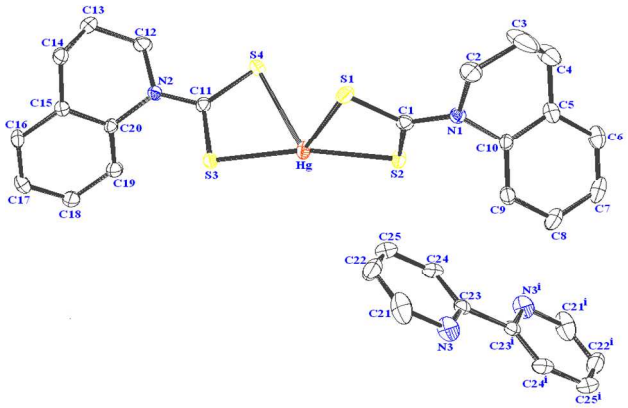

$[Hg(thqdtc)_2] \cdot 0.5(2,2'\text{-bipy})$

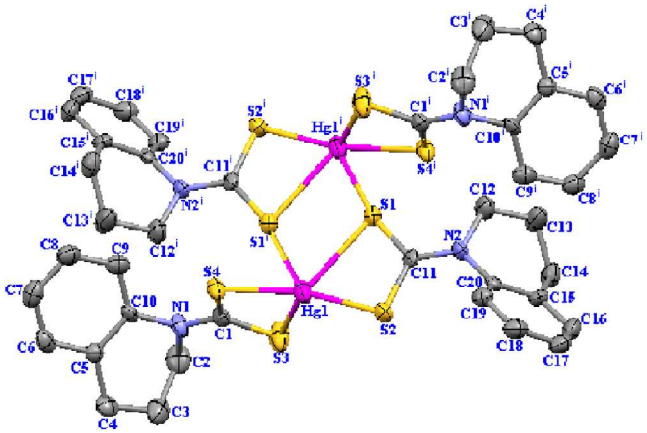

$[Hg(thqdtc)_2] \cdot 0.25C_2H_5OH$

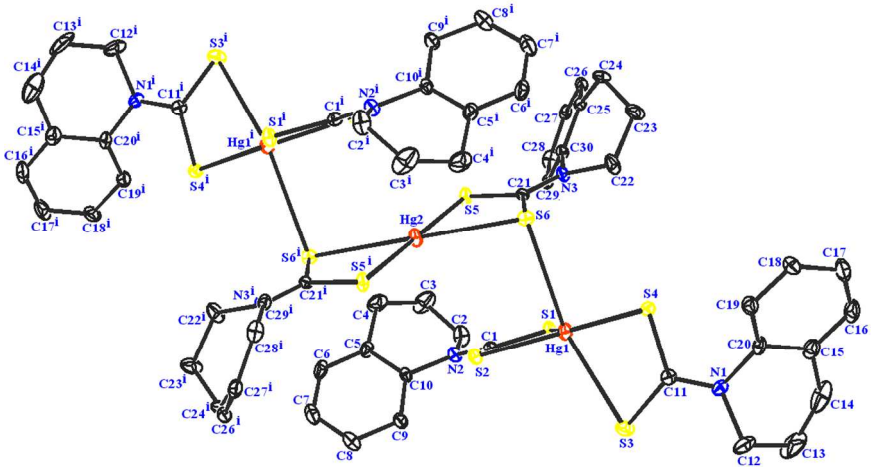

$[Hg_3(thqdtc)_6] \cdot py$